Dynamic Light Scattering Study of Calmodulin–Target Peptide Complexes

Andriyka L. Papish, Leslie W. Tari, and Hans J. Vogel
Structural Biology Research Group, Department of Biological Sciences, University of Calgary, Calgary, Alberta T2N 1N4, Canada

ABSTRACT Dynamic light scattering (DLS) has been used to assess the influence of eleven different synthetic peptides, comprising the calmodulin (CaM)-binding domains of various CaM-binding proteins, on the structure of apo-CaM (calcium-free) and Ca^{2+}-CaM. Peptides that bind CaM in a 1:1 and 2:1 peptide-to-protein ratio were studied, as were solutions of CaM bound simultaneously to two different peptides. DLS was also used to investigate the effect of Ca^{2+} on the N- and C-terminal CaM fragments TR1C and TR2C, and to determine whether the two lobes of CaM interact in solution. The results obtained in this study were comparable to similar solution studies performed for some of these peptides using small-angle x-ray scattering. The addition of Ca^{2+} to apo-CaM increased the hydrodynamic radius from 2.5 to 3.0 nm. The peptides studied induced a collapse of the elongated Ca^{2+}-CaM structure to a more globular form, decreasing its hydrodynamic radius by an average of 25%. None of the peptides had an effect on the conformation of apo-CaM, indicating that either most of the peptides did not interact with apo-CaM, or if bound, they did not cause a large conformational change. The hydrodynamic radii of TR1C and TR2C CaM fragments were not significantly affected by the addition of Ca^{2+}. The addition of a target peptide and Ca^{2+} to the two fragments of CaM, suggest that a globular complex is forming, as has been seen in nuclear magnetic resonance solution studies. This work demonstrates that dynamic light scattering is an inexpensive and efficient technique for assessing large-scale conformational changes that take place in calmodulin and related proteins upon binding of Ca^{2+} ions and peptides, and provides a qualitative picture of how this occurs. This work also illustrates that DLS provides a rapid screening method for identifying new CaM targets.

INTRODUCTION

Calmodulin (CaM) is a small, acidic intracellular calcium receptor protein that has been studied extensively. This ubiquitous protein is implicated in the regulation of many Ca^{2+} dependent-signaling pathways in eukaryotic cells, and is a well-known secondary messenger (Vogel, 1994; James et al., 1995; Ikura, 1996). It consists of 148 amino acid residues arranged in the shape of a dumbbell, with two globular domains joined by a flexible central linker region. Crystal structures indicate that the linker region of Ca^{2+}-CaM is α-helical (Babu et al., 1988) but nuclear magnetic resonance (NMR) spectroscopy studies show that the central part of this linker region is unstructured in solution (Barbato et al., 1992). The apo structure of CaM reveals a reorientation of the α-helices within each lobe. However, the overall flexible dumbbell structure is preserved (Kuboniwa et al., 1995; Zhang et al., 1995a). Each domain or lobe of CaM comprises two helix-loop-helix motifs (EF hands) with the potential to bind two Ca^{2+} ions per lobe (Fig. 1 *A*). A small β-sheet connects the two Ca^{2+} binding loops. Calcium ions bind with the highest affinity to the carboxy (C)-terminal domain ($K_d = 10^{-7}$ M) and more weakly to the amino (N)-terminal lobe ($K_d = 10^{-6}$ M) (Thulin et al., 1984; Vogel, 1994; James et al., 1995). The binding of the Ca^{2+} ions causes a large conformational change resulting in elongation of CaM in solution (Seaton et al., 1985) and the exposure of two hydrophobic patches, one centered on the concave surface of each cup-shaped lobe (Crivici and Ikura, 1995; Yuan et al., 1999a). These hydrophobic patches play an integral role in the binding of CaM to its target proteins and peptides, along with the negatively charged residues at the rims of the lobes (O'Neil and DeGrado, 1990). The majority of the CaM-binding domains of CaM-binding target proteins are short contiguous regions, 15–30 amino acids in length, that have a propensity to form basic amphiphilic α-helices (Vogel and Zhang, 1995; Crivici and Ikura, 1995). When bound to Ca^{2+}-CaM, generally in a 1:1 complex, these targets induce a collapse of the dumbbell-shaped CaM structure around the target, causing it to form a compact globular structure (Fig. 1 *B*) and activating the CaM-binding protein. Two notable exceptions are peptides derived from the CaM-binding domains of caldesmon (CaD) and a peptide encompassing the C-terminal region of petunia glutamate decarboxylase (PGD). The CaD peptides are distinctive in that two different peptides can bind to Ca^{2+}-CaM simultaneously (Zhou et al., 1997; Krueger et al., 2000). The PGD peptide is unusual because it forms a 2:1 peptide–protein complex with Ca^{2+}-CaM, and it is also atypical because it contains five negatively charged residues (Yuan and Vogel, 1998). In certain cases, two CaM molecules may be required for the activation of the CaM target protein. This is exemplified by the CaM binding domains of small-conductance Ca^{2+}- activated K^+ membrane channels, which require the binding of two CaM molecules for the modulation of the gating mechanism (Schumacher et al., 2001). Most target proteins are not activated in the absence of Ca^{2+} (Crivici and Ikura, 1995). The CaM-binding proteins tend to be quite large and multimeric, making it often difficult

Submitted September 27, 2001 and accepted for publication May 23, 2002.

Dr. Tari's present address is Syrrx Inc., San Diego, CA.

Address reprint requests to Hans J. Vogel, Structural Biology Research Group, Dept. of Biological Sciences, Univ. of Calgary, Calgary, AB T2N 1N4, Canada. Tel.: 403-220-6006; Fax: 403-289-9311; E-mail: vogel@ucalgary.ca.

0006-3495/02/09/1455/10 $2.00

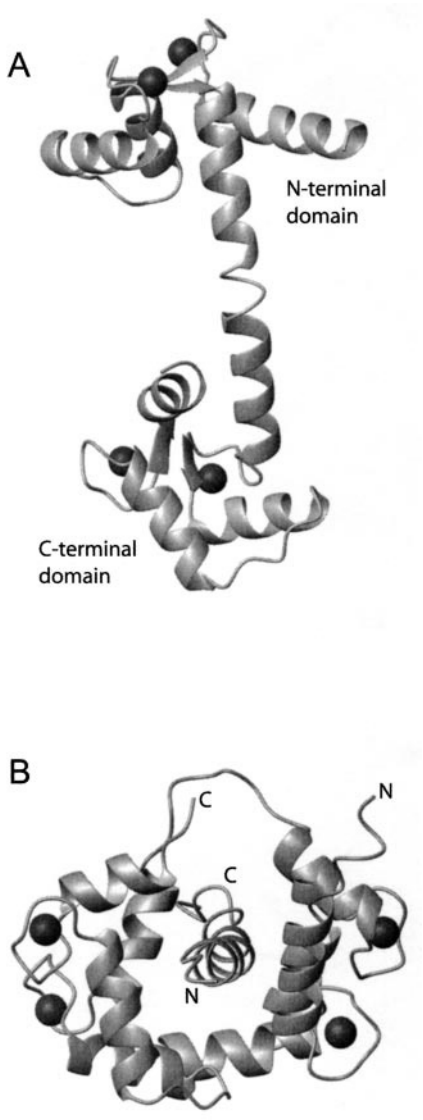

FIGURE 1 (*A*) X-ray structure of Ca^{2+}-CaM determined at 2.2-Å resolution by Babu et al., 1988. (3CLN). (*B*) NMR structure of the complex of Ca^{2+}-CaM with the skMLCK peptide. The hydrophobic channel formed by the terminal domains of CaM that enclose the target peptide is shown (2BBM).

to study their interaction with CaM at the molecular level. For this reason, synthetic peptides comprising the CaM-binding domain of the proteins are useful substitutes to study the interaction of CaM with its targets. In many instances it has been shown that the affinity of CaM for the peptide and the target protein from which it is derived is very similar (Vogel, 1994; Crivici and Ikura, 1995).

Calmodulin–peptide interactions

To date, over 80 different CaM targets have been identified, including protein kinases and phosphatases (e.g., calmodulin-dependent protein kinases I and II (CaMKI, CaMKII), skeletal–muscle myosin light chain kinase (skMLCK), smooth-muscle myosin light chain kinase (smMLCK) and calcineurin) and proteins involved in the regulation and generation of second messengers, such as nitric oxide synthases and cyclic nucleotide phosphodiesterase (PDE) (Vogel, 1994; Vogel and Zhang, 1995). Although most CaM target peptides are hydrophobic and basic, they possess no significant amino acid sequence homology. Ca^{2+}-CaM is capable of binding a diverse range of peptides with very high affinity ($K_d = 10^{-7}$ M to $K_d = 10^{-11}$ M) (Crivici and Ikura, 1995). Several features intrinsic to CaM are believed to be important for peptide binding. The first structural characteristic of CaM crucial for the association of Ca^{2+}-CaM with peptides is the flexibility of its α-helical linker region. This interconnecting region acts as a hinge, enabling the two globular lobes of CaM to wrap around targets of diverse lengths and dimensions, to varying degrees (Crivici and Ikura, 1995). It is also capable of unwinding to differing extents to facilitate binding with various target proteins. The distance between the two lobes of CaM is dependent upon the positioning of the hydrophobic anchors on the target peptide and upon the length of the peptide helix. Another key property of CaM is its unusually high content of methionine (Met) residues (9 in total). Met residues are flexible and hydrophobic, and contain a highly polarizable sulfur atom. Met residues can readily adjust their conformations to optimize the binding of the different target α-helices via hydrophobic interactions (Gellman, 1991; Yuan et al., 1999a). Though the interactions between the peptide and CaM are primarily hydrophobic in nature, electrostatic interactions also play a significant role. This is evident from the interactions between several glutamic acid residues of both the N- and C-terminal domains of CaM with the basic residues of the target, forming salt bridges (Ikura et al., 1992).

Calmodulin-peptide complexes, CaM fragments and light scattering

Various studies have been conducted regarding Ca^{2+}-CaM–peptide interactions. Structures of the skMLCK and CaM-dependent protein kinase kinase peptides complexed with Ca^{2+}-CaM have been solved using NMR (Ikura et al., 1992; Osawa et al., 1999), whereas the structures of the smMLCK and the CaMKII peptide fragments complexed with Ca^{2+}-CaM have been solved by x-ray crystallography (Meador et al., 1992, 1993). Additionally, a number of CaM-peptide complexes and a CaM-protein complex have been studied using small-angle x-ray or neutron scattering (SAXS), demonstrating that SAXS is an excellent tool for obtaining detailed structural information (Seaton et al., 1985; Trewhella et al., 1990; Kataoka et al., 1991; Yoshino et al., 1993, 1996; Trewhella, 1997; Trewhella and Krueger, 2001; Izumi et al., 2001).

Recently, a noninvasive and nondestructive technique has gained popularity for exploring size and shape properties of macromolecules in solution (Murphy, 1997). Dynamic light

scattering (DLS) is a technique that measures the diffusion coefficient of a particle in solution and hence the hydrodynamic radius obtained from DLS is generally calculated based on a spherical approximation. The major advantages of light scattering over other techniques yielding structural information include the extremely short time required to obtain data, the modest amounts of protein required (1–10 mg/mL) in very small sample volumes (12 μL per cuvette), and its relative simplicity and accessibility to most researchers. Structural information about particles 1–1000 nm in size can be obtained (Murphy, 1997). The primary concern with light scattering is that it is extremely sensitive to small amounts of aggregation or the presence of dust particles. The strength of DLS is its ability to act as a rapid screen of major conformational changes in proteins or protein complexes in solution. These proteins can then be further evaluated by techniques such as NMR or SAXS, which provide more detailed shape and structural information.

In this work, DLS was used to examine several CaM–peptide complexes, as well as the two CaM fragments TR1C (residues 1–75) and TR2C (residues 78–148). Combinations of the CaM fragments were also studied in the presence and absence of the CaMKI peptide. The hydrodynamic radius of each complex or fragment was determined both in the absence (apo form) and presence of Ca^{2+}. Eleven different synthetic peptides were used, each representing the CaM-binding region of different CaM-binding proteins. Such peptides are known to form complexes with CaM that closely resemble its interaction with the intact target proteins, as has been demonstrated for CaMKI, for example (Gomes et al., 2000; Kranz et al., 2002). The eleven peptides used in this study can be divided into three classes, based on the stoichiometry of their interactions with CaM. The first class consists of seven peptides, which bind CaM in a 1:1 ratio. These peptides correspond to the CaM binding regions of skMLCK (Ikura et al., 1992; Zhang et al., 1993), constitutive nitric oxide synthase (Zhang and Vogel, 1994; Zhang et al., 1995b), PDE (Yuan et al., 1999b), simian immunodeficiency virus glycoprotein gp41 (C837S) (Yuan et al., 1995; Yuan et al., 2001) and CamKI (Gomes et al., 2000), and include the N- and C-terminal segments of melittin, MLN and MLC (Yuan et al., 2002, submitted for publication). The three fragments derived from the two CaM binding domains of the protein CaD make up the second class. These peptides not only bind CaM in a 1:1 ratio, but the different fragments may be capable of binding CaM simultaneously (Zhou et al., 1997, Krueger et al., 2000). A third class of CaM–peptide interactions comprises a peptide from the CaM binding region of the C-terminus from PGD. The PGD peptide is unique in that it forms a 1:2 protein–peptide complex with CaM (Yuan and Vogel, 1998).

The aim of this work was to investigate the conformational changes in CaM when bound to these various peptides in the presence and absence of Ca^{2+}. We have also used DLS to study potential interactions of proteolytic fragments of CaM in solution. This work is significant because it portrays a qualitative picture of how the conformation of CaM is changing upon binding to target peptides. This characteristic alteration that occurs in CaM upon binding to its targets demonstrates that DLS can be used as a rapid screen for CaM targets. This work is also important because it illustrates that DLS can be successfully applied to study peptides that utilize novel stoichiometry and can therefore be used to study multiple binding sites on proteins.

MATERIALS AND METHODS

Protein Purification

Calmodulin was cloned and overexpressed from the *Escherichia coli* strain MM294 (obtained from the *E. coli* genetic stock center at Yale University) transformed with the temperature-sensitive pCaM plasmid (from Dr. T. Grundström, University of Umea, Sweden). Purification of CaM was performed as described by Zhang and Vogel (1993), using calcium-dependent chromatography on phenyl-Sepharose (Vogel et al., 1983). The purity was assessed using SDS-polyacrylamide gel electrophoresis (4% stacking gel, 15% separating gel), and its concentration was determined using the absorption coefficient of $\epsilon_{276}^{1\%} = 1.8$. The TR1C fragment, consisting of residues 1–75 of CaM, was cloned and overexpressed from *E. coli*, whereas the TR2C fragment (residues 78–148) was obtained by trypsin digestion of CaM (Vogel et al., 1983; Fabian et al., 1996).

Peptides

The majority of the peptides were custom synthesized at the Peptide Synthesis Facility at Queen's University, (Kingston, ON, Canada), with the exception of C837S and PGD. They were >95% pure as judged by HPLC. The mass spectrum of all the peptides agreed to within one Da of the expected mass. C837S was obtained from the Peptide Synthesis Facility at the University of Pittsburgh (Pittsburgh, PA), whereas the PGD peptide was purchased from the University of Calgary Peptide Synthesis Facility (Calgary, AB, Canada). Their amino acid sequences and protein origins are listed in Table 1.

Sample preparation for static light scattering and data acquisition

To determine the aggregation state of CaM in solution, CaM solutions of varying concentrations were prepared and analyzed by static light scattering. Apo-CaM was dissolved in a solution of 100 mM Tris-HCl, 100 mM KCl at pH 7.4. The 8.4 mg/ml stock solution of apo-CaM was then diluted with a 100 mM Tris-HCl, 100 mM KCl (pH 7.4) buffer, resulting in CaM concentrations of 6.9, 6.7, 5.9, 5.0, 4.2, 3.4, 2.5, and 1.3 mg/ml. Each sample was passed through a 0.02-μm, 13-mm Whatman anodisc and 12 μL was loaded into a quartz cuvette, then placed into the DynaPro MSTC light scattering instrument. Laser light with a wavelength of 827.6 nm was used, and intensities were measured at an angle of 90°. Data were collected at 20°C, and then analyzed using a Zimm plot as implemented in the DynaPro static light scattering software (DYNAMICS). Toluene was used as a reference. A refractive index increment of the sample molecules (dn/dc) of 0.19 was used, and the partial specific volume of CaM used was 0.73 mL/g (Squire and Himmel, 1979), a value typical of globular proteins. CaM has a theoretical molecular weight of 16,702.

Sample preparation for dynamic light scattering

Several different CaM-peptide solutions were prepared and analyzed by DLS. The apo-CaM + peptide solutions contained stoichiometric ratios of

TABLE 1 Amino acid sequences for the peptides composed of the CaM-binding domains of CaM binding proteins

Peptide	Peptide Sequence	Mw, (Da)	Corresponds to CaM-binding domain of:
CaD 1	GVRNIKSMWEKGNVFSSC	2040.98	First CaM-binding domain of CaD
CaD 2A	NKETAGLKVGVSSRINEWLTKTC-NH2	2532.32	Second CaM-binding domain of CaD
CaD 2B	SRINEWLTK-NH2	1186.6	Part of second CaM-binding domain of CaD
PDE	AcQTEKMWQRLKGILRCLVKQL-NH2	2511.43	Bovine brain PDE1A2
skMLCK	KRRWKKNFIAVSAANRFKKISS	2634.53	Skeletal myosin light chain kinase
CaMK1	AKSKWKQAFNATAVVRHMRKLQ	2597.45	Rat brain CaM-dependent protein kinase I
MLN	GIGAVLKVLTTGL	1660	N-terminus of Melittin
MLC	Ac-PALISWIKRKRQQ	1664.94	C-terminus of Melittin
cNOS	KRRAIGFKKLAEAVKFSAKLMQG	2576.47	Constitutive nitric oxide synthase
C837S	DLWETLRRGGRWILAIPRRIRQGLELTL-NH2	3220	SIV transmembrane glycoprotein gp41 (Cys to Ser mutant)
PGD	HKKTDSEVQLENITAWKKFVEEKKKK	3188.8	Carboxy-terminal domain from petunia glutamate decarboxylase

protein to peptide, with a CaM concentration of 7.3 mg/ml and 2 mM EDTA. The Ca^{2+}-CaM plus peptide solutions also contained stoichiometric ratios of protein to peptide, with a CaM concentration of 7.3 mg/ml and 10 equivalents of Ca^{2+}. In the case of PGD, which binds CaM in a ratio of 2:1 peptide to protein, two and three equivalents of peptide were also added to Ca^{2+}-CaM. The solutions containing CaD and PGD peptides also contained 1 mM dithiothreitol to prevent oxidation of the cysteine residues in these peptides. Samples were also prepared that contained two different CaD peptides; one equivalent of each CaD peptide and one equivalent of CaM. Solutions of apo-CaM and Ca^{2+}-CaM were prepared as above but without the addition of peptides. The TR1C and TR2C fragments were dissolved in 100 mM Tris-HCl, 100 mM KCl to a concentration of 8.5 mg/ml, pH 7.4. The apo samples contained 2 mM EDTA, whereas the Ca^{2+} samples contained ten equivalents of $CaCl_2$. Apo and Ca^{2+} samples with one equivalent of each fragment were also prepared, as were solutions with one equivalent of CaMKI peptide in the presence of both fragments. As in static light scattering, samples were passed through a 0.02-μm, 13-mm Whatman anodisc filter, loading 12 μL into a quartz cuvette, then placed into the DynaPro MSTC dynamic light scattering instrument. Approximately 100 measurements were collected for each of three to four independently prepared samples at 20°C by the DynaPro MSTC instrument. Samples that were not passed through the 0.02-μm filter or which contained remaining dust particles resulted in large fluctuations in the instrument readings, and it was not possible to collect useful data for such samples. Such measurements were repeated with samples providing stable measurements. Thus the influence of dust as a contributing factor to the radius of the sample was assumed to be negligible. The data was analyzed to obtain the hydrodynamic radius (R_H) values for each sample. The standard deviations for the radii were calculated, and are an error estimate of the hydrodynamic radius of the molecule in solution, based on multiple samples. The reported R_H values are the mean size of the dominant peak.

Static light scattering data analysis

Static light scattering is based on the principle of Rayleigh light scattering, and can be used to obtain a weight-averaged molecular weight of the species in solution. The Rayleigh ratio describes the absolute intensity scattered at an angle θ in excess of the light scattered by the pure solvent, and is described by

$$R(\theta) = I_{scat} r^2 / I_{incid}(1 + \cos^2\theta), \quad (1)$$

where I is intensity (van Holde et al., 1998), and $R(\theta)$ is a function of both R_g (radius of gyration) and molecular weight. From Eq. 2, the average molecular weight of the protein or molecule in solution can be determined using a Zimm plot, where $KC/R(\theta)$ is plotted against the concentration, C, in mg/ml,

$$KC/R(\theta) = 1/P(\theta)\ \mathrm{Mw} + 2BC, \quad (2)$$

where $K = 4\pi^2 n^2 (dn/dc)^2/N\lambda^4$ (Murphy, 1997). The refractive index of the solvent is n, dn/dc is the change in the refractive index with change in concentration, N is Avogadro's number and λ is the wavelength. $P(\theta)$ represents the particle shape factor, Mw is the weight-averaged molecular weight of particles in solution, B is the second viral coefficient, which is a collection of constants including R_g, and C is the concentration. As long as the particle size is less than 10% of the wavelength of the incoming radiation, the molecular weight obtained is unaffected by molecular shape.

Dynamic light scattering data analysis

In DLS, a monochromatic beam of light of 827.6 nm illuminates the cuvette containing the sample, and the fluctuation of intensity in the scattered light (microsecond timescale) is detected by the photo diode at 90° (Murphy, 1997). The position of the particles relative to the detector influences the scattering intensity measured by the detector. In the absence of any applied forces, the change in the position of a particle is determined by the degree of simple Brownian motion. An autocorrelator is used to analyze the fluctuations in scattering by performing Fourier analysis of these fluctuations (van Holde et al., 1998), giving the normalized first-order autocorrelation function, $G(\tau)$, from which D_T is obtained (Murphy, 1997),

$$G(\tau) = 1 + \exp(-2D_T q^2 \tau). \quad (3)$$

D_T is the translational diffusion coefficient of the molecule and, $q = (4\pi n/\lambda)\sin(\theta/2)$. The refractive index of the solvent is n, θ is the scattering angle, and λ is the wavelength of incident light. It is assumed that particles undergo simple Brownian motion. D_T is inversely proportional to the frictional coefficient for any shape, f, which depends on molecular size,

$$D_T = RT/Nf, \quad (4)$$

where RT is a measure of thermal energy and N is Avogadro's number.

Once D_T is known, the hydrodynamic radius (R_H) can be obtained from the Stokes–Einstein equation,

$$D_T = k_B T/6\pi\eta R_H, \quad (5)$$

where k_B is the Boltzmann constant, T is the temperature in Kelvin, η represents the viscosity of the solvent, and R_H is the hydrodynamic radius of the average scattering molecule. Thus, DLS is used to obtain an indirect measurement of R_H, which is a spherical approximation of the radius of the molecule in solution.

RESULTS AND DISCUSSION

Static and dynamic light scattering of CaM

To ensure that calmodulin was monomeric at the concentrations used throughout this study, a Zimm plot was ob-

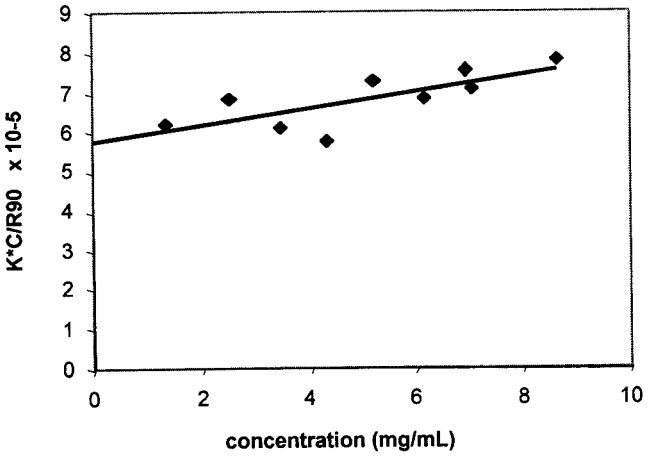

FIGURE 2 Zimm plot of apo-CaM. Molecular weight = 16.7.

tained (Fig. 2). A molecular weight for CaM of 16.7 was obtained from the Zimm plot, indicating that, in the range of 1.30–8.39 mg/ml, CaM was monomeric. This result was not unexpected, because Seaton et al., (1985) found that CaM does not exhibit any concentration-dependent aggregation in the 8.7–37.1 mg/ml range for apo-CaM, nor in the 9.1–36.1 mg/ml range for Ca^{2+}-CaM. The theoretical molecular weight of recombinant CaM is 16.702, and was confirmed for our CaM preparation by electrospray mass spectrometry (data not shown).

Various trends observed using DLS were similar to those obtained in SAXS and NMR studies (Seaton et al., 1985; Vogel, 1994). DLS results for Ca^{2+}-CaM show that its hydrodynamic radius (R_H) is 3.0 nm (Table 2), which corresponds to a diameter of 6.0 nm. This is very similar to the maximum vector length (d_{max}) obtained by Seaton et al. (1985) of 6.2 nm, using SAXS. The R_H obtained for apo-CaM by DLS was 2.5 nm (Table 2), yielding a diameter of 5.0 nm. This is somewhat smaller than the d_{max} of 5.8 nm obtained by Seaton et al. (1985). The SAXS study indicates a 6.5% difference in overall diameter between Ca^{2+}-CaM and apo-CaM, whereas a difference of 16.7% was found using DLS. Although the two methods yield similar information, it is important to recall that the d_{max} measured using SAXS is a measure of the maximum distance between two scattering centers of the molecule, whereas the R_H obtained using DLS is a spherical approximation of the radius and is obtained via indirect measurement of the radius. This difference in the specific properties measured by the two techniques most likely accounts for the variation in the values obtained. It is also possible that the extent of hydration in CaM differs between Ca^{2+} and apo-CaM, accounting for the greater difference when using DLS.

TABLE 2 Dynamic light scattering results for Apo and Ca^{2+} calmodulin in the presence of peptides

	Apo		Ca^{2+}	
Peptide	RH*	(SD)	RH	(SD)
CaM	2.5	(0.1)	3.0	(0.1)
CaMK1	2.5	(0.1)	2.2	(0.1)
PDE	2.5	(0.1)	2.3	(0.1)
MLCK	2.5	(0.1)	2.2	(0.1)
cNOS	2.5	(0.1)	2.3	(0.1)
C837S	2.5	(0.1)	2.4	(0.2)
MLC	2.5	(0.1)	2.3	(0.1)
MLN	2.5	(0.1)	2.2	(0.1)
CaD1	2.6	(1.0)	2.4	(0.2)
CaD2A	2.5	(0.2)	2.4	(0.1)
CaD2B	2.5	(0.1)	2.7	(0.1)
CaD1/CaD2A	2.6	(0.2)	2.3	(0.2)
CaD1/CaD2B	2.5	(0.1)	2.3	(0.2)
ONE X PGD	2.5	(0.1)	2.8	(0.1)
TWO X PGD	–		2.5	(0.1)
THREE X PGD	–		2.4	(0.1)

*RH, hydrodynamic radius (nm); SD, standard deviation.

DLS of 1:1 Calmodulin-peptide complexes

The binding of the skMLCK and smMLCK peptide to Ca^{2+}-CaM has been widely accepted as a model for the interaction of Ca^{2+}-CaM with peptides (Ikura et al., 1992; Meador et al., 1992). When the skMLCK peptide is bound to Ca^{2+}-CaM, the elongated CaM structure collapses around the peptide, resulting in a more globular shape (Fig. 1 *B*). However, the skMLCK peptide does not induce a change in CaM when Ca^{2+} is absent. Because the majority of CaM's target proteins are inactive when Ca^{2+}-CaM is absent (Vogel, 1994), it is not surprising that the presence of CaM-binding peptides in solution has little effect on the R_H of apo-CaM. In contrast, if the peptides bind to and alter the conformation of Ca^{2+}-CaM in a fashion similar to what is observed for the skMLCK peptide, then significant changes in the R_H of Ca^{2+}-CaM would be expected.

Several peptides were studied that bind Ca^{2+}-CaM in a 1:1 ratio. They are all derived from proteins whose CaM-binding domain is believed to be one contiguous region in the amino acid sequence. Each of these peptides decreased the R_H of Ca^{2+}-CaM by approximately 25% (Table 2), consistent with a collapse of the elongated dumbbell structure to a more globular form. This includes the skMLCK peptide, which decreased the R_H of Ca^{2+}-CaM from 3.0 to 2.2 nm—a result comparable to the SAXS studies reported by Heidorn et al., (1989). These indicated that the skMLCK peptide–Ca^{2+}-CaM complex was 20% smaller than Ca^{2+}-CaM, compared to a 25% decrease using DLS. The structural collapse of the skMLCK peptide–CaM complex is also clearly evident for the NMR solution structure (Ikura et al., 1992). The CamKI peptide–complex (R_H = 2.2 nm) and the MLN complex (R_H = 2.2 nm) also showed significant conformational changes compared to the control (R_H = 3.0 nm). These results suggest that the Ca^{2+}-CaM/CaMKI complex and the Ca^{2+}-CaM/MLN are nearly spherical, as is the case for the skMLCK peptide–Ca^{2+}-CaM complex (Ikura et

al., 1992). The MLC peptide, the PDE, the constitutive nitric oxide synthase peptide, and the C837S peptide, corresponding to the CaM-binding domain of the simian immunodeficiency virus, all affected the shape of Ca^{2+}-CaM similarly by decreasing R_H by ~25%. No correlation was found between the R_H of the complexes and either the length of the peptides or the relative positions of hydrophobic anchor residues in the sequence of the peptides. Figure 3 shows representative data for Ca^{2+}-CaM, PDE in a solution of apo-CaM and the Ca^{2+}-CaM–PDE complex. For all peptide complexes, it was noted that the width of the major peak was markedly reduced upon peptide binding (compare panel Fig. 3 *C* to Fig. 3, *A* and *B*). This suggests the formation of a well-defined complex, whereas, for apo-CaM and Ca^{2+}-CaM, a distribution of R_H may exist in solution, in agreement with NMR solution data (Barbato et al., 1992).

A recent study by Brokx et al. (2001) found that several CaM-binding peptides could be separated into two groups according to the change in heat capacity (ΔCp) upon complex formation with Ca^{2+}-CaM. They concluded that certain peptides, such as CaMKI, which exhibited ΔCp values around -3.2 kJ·mol^{-1}K^{-1}, were forming CaM–peptide complexes in the canonical fashion, whereas complexes with ΔCp values around -1.6 kJ·mol^{-1}K^{-1} exemplified interactions between the peptide and primarily the C lobe of Ca^{2+}-CaM. The latter included the PDE and MLC peptides. Thus, the differences in the amount of decrease in R_H exhibited by the binding of the CaMKI peptide to Ca^{2+}-CaM as compared to the binding of the PDE and MLC peptides, may be due to differing interactions in the formation of the peptide–Ca^{2+}-CaM complexes.

DLS of Caldesmon–Calmodulin interactions

It has been suggested that CaD may contain two distinct CaM-binding domains, and that these may bind simultaneously to Ca^{2+}-CaM (Marston et al., 1994; Mezgueldi et al., 1994; Wang et al., 1997; Zhou et al., 1997). This prediction was investigated using DLS. The peptide corresponding to the first CaM-binding domain of CaD (CaD1) and the peptide corresponding to the second CaM-binding domain of CaD (CaD2A) individually imposed an identical decrease in R_H upon binding Ca^{2+}-CaM (20.0%) (Table 2). This was in contrast to the CaD2B peptide, corresponding to the N-terminal region of the second CaM-binding domain of CaD. CaD2B had a much smaller effect on R_H in Ca^{2+}-CaM (10.0%). The R_H (2.7 nm) was almost at the midpoint of Ca^{2+}-CaM (3.0 nm) and apo-CaM (2.5 nm), suggesting that CaD2B only binds weakly to CaM.

The combination the CaD2B peptide with CaD1 produced a greater decrease in the R_H of Ca^{2+}-CaM than did the CaD2B peptide alone. This combination induced a conformational change similar to what was observed in the 1:1 peptide–Ca^{2+}-CaM complexes studied (Table 2). The presence of both the CaD1 and the CaD2A peptides with Ca^{2+}-CaM resulted in an R_H value of 2.3 nm, as did the addition of CaD1 and CaD2B to Ca^{2+}-CaM. These results suggest that both CaM-binding domains of CaD may be binding simultaneously to Ca^{2+}-CaM to form a collapsed structure. Although results from studies by Zhou et al. (1997) are consistent with this hypothesis, SAXS studies by Krueger et al. (2000) found that CaM remains extended upon binding of CaD peptides containing two CaM binding sites. This

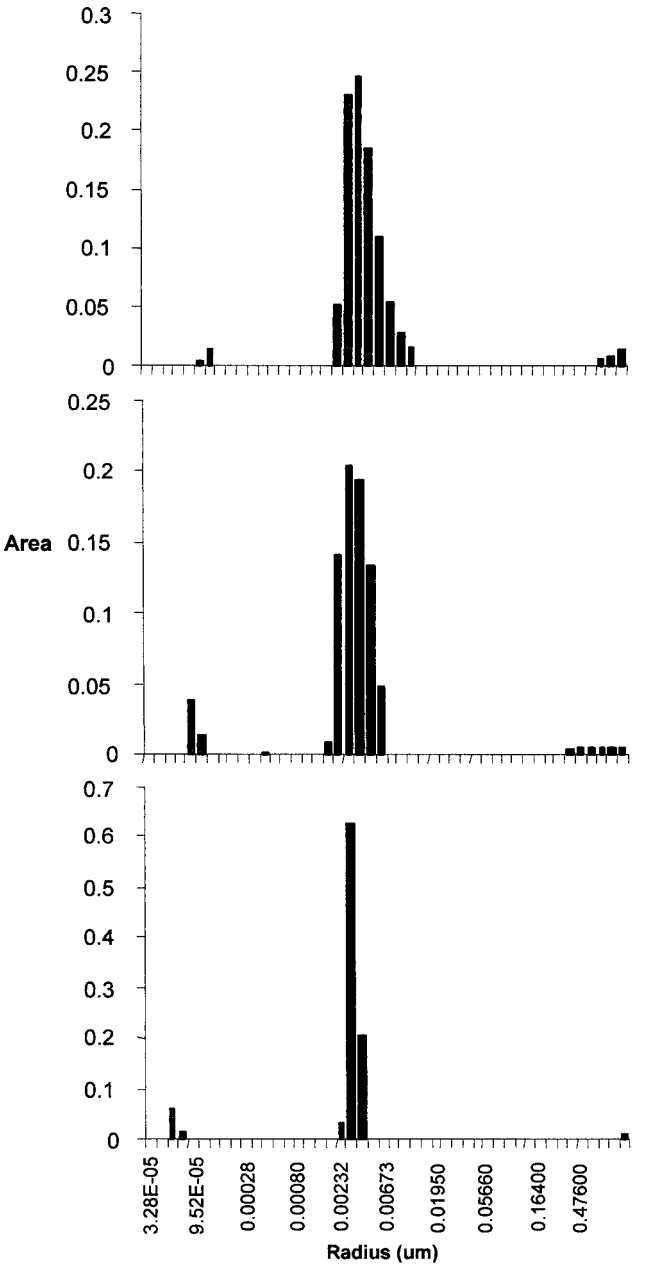

FIGURE 3 Size distribution histogram for: (*A*) Ca^{2+}-CaM; (*B*) PDE peptide in a solution of apo-CaM; (*C*) PDE peptide in a solution of Ca^{2+}-CaM. Notice the increased monodispersity of *C* as opposed to *A* and *B*, as illustrated by the sharpening of the distribution.

discrepancy may be due to the binding of one peptide with two CaM binding sites, as in the SAXS study, versus the binding of two separate peptides to CaM, as in the DLS study. The presence of only one peptide extending both CaM binding sites may hinder the formation of a globular complex, whereas the binding of two separate CaD peptides to Ca^{2+}-CaM does not.

Another inference that can be made from the DLS data is that the CaD2A and CaD1 peptides impart a far greater conformational change on Ca^{2+}-CaM than does the CaD2B peptide (Table 2). This is in agreement with results obtained by Zhou et al., (1997) which indicate a higher binding affinity for CaD2A to CaM than for CaD2B. The greater conformational change associated with these peptides is most likely due to electrostatic interactions between the N-terminal region of CaD2A and acidic CaM residues, as well as hydrophobic interactions between CaD1 and CaM.

1:2 Calmodulin–PGD peptide interactions

Previous work by Yuan and Vogel (1998) has shown that the 26-residue peptide derived from the CaM-binding domain in the C-terminus of PGD is capable of binding Ca^{2+}-CaM in a 2:1 peptide–protein ratio, which is a novel mode for peptide binding to CaM. The DLS results support this notion (Table 2), and provide further evidence illustrating the usefulness of DLS as a rapid method for obtaining information regarding the binding of CaM with its targets. The addition of one molar equivalent of the PGD peptide to Ca^{2+}-CaM had only a minor effect on the R_H of Ca^{2+}-CaM (2.8 versus 3.0 nm for Ca^{2+}-CaM). However, the addition of up to two equivalents of the PGD peptide to a solution of Ca^{2+}-CaM apparently completes the formation of the complex and resulted in a dramatic decrease in the width of the major peak in the distribution histogram and the hydrodynamic radius of the complex (Fig. 4). Again, we suggest that the width of the distribution histogram denotes the spread of the particle sizes about the R_H. The binding of the two peptides is believed to be simultaneous (Yuan and Vogel, 1998), which is consistent with this profile. Although the R_H of this complex (2.5 nm) is slightly larger than for Ca^{2+}-CaM complexed to the other peptides (with the exception of CaD2B), it is likely due to the presence of two PGD peptides bound to Ca^{2+}-CaM. Despite the five negatively charged residues in the PGD peptide, a 20% decrease in the R_H of Ca^{2+}-CaM was still seen. These residues would be expected to hinder the binding of the peptide to the acidic CaM protein. By comparison, the other peptides that were studied here are all basic in nature. Yuan and Vogel (1998) suggest that ion pairs could be forming at the peptide dimer interface, allowing for the interaction of the hydrophobic portions of the PGD monomers with the Met-rich surfaces of Ca^{2+}-CaM. The size distribution histograms for PGD binding to CaM (Fig. 4) support this prediction. The distribution in Fig. 4 *B* suggests the presence of both unbound Ca^{2+}-CaM and the 2-PGD–Ca^{2+}-CaM complex in solution, whereas Fig. 4 *C* clearly indicates the presence of only one species, the 2-PGD–Ca^{2+}-CaM complex. The addition of a third equivalent of the PGD peptide did not have a significant effect on the complex (Fig. 4 *D*). These results clearly indicate that PGD can bind to Ca^{2+}-CaM in a 2:1 ratio in a rigid, compact globular complex.

Apo-Calmodulin complexes and DLS

The DLS results in Table 2 (apo-CaM plus peptides and apo-CaM plus CaD peptides) indicate that, for all thirteen samples investigated, very little deviation was seen in the R_H values for apo-CaM in the presence of a peptide. The R_H values in the presence of the peptides were all within $\pm 4\%$ of the apo-CaM control value of 2.5 nm (Table 2). This endorses the hypothesis that most of these peptides are not binding apo-CaM or are only weakly binding but not modifying the conformation of apo-CaM at 100 mM salt concentrations.

Yuan et al. (1999b) performed NMR, circular dichroism, and Fourier transfer infrared spectroscopy experiments that demonstrated that the PDE peptide is capable of binding to the C-terminal domain of apo-CaM at physiological salt concentrations as a partial α-helix with some β-turn structure. They suggested that the C-terminal lobe of the apo-CaM peptide complex adopt a partially open conformation, while the N-terminal lobe remains completely closed. The existence of this apo-CaM–PDE peptide complex was recently confirmed by SAXS measurements of the complex (H. Yoshino and H. J. Vogel, unpublished results; see also Izumi et al., 2001). The results for the PDE peptide, with an R_H value of 2.5 when in the presence of apo-CaM, follow the same trend as the other solutions of peptides and apo-CaM. Thus binding of the PDE peptide to the C-terminal domain of apo-CaM does not give rise to any large changes in the overall structure of apo-CaM.

Calmodulin fragments TR1C and TR2C

The two domains of CaM can be studied separately by performing DLS measurements on the two CaM fragments TR1C and TR2C, allowing the study of the interaction of the two CaM domains. The N-terminal fragment of CaM, TR1C, consists of amino acids 1–75, whereas TR2C, the C-terminal fragment, encompasses residues 78–148 of CaM. Various studies (e.g., Vogel et al., 1983, Thulin et al., 1984; Finn et al., 1993; Fabian et al., 1996) have demonstrated that the secondary and tertiary structures of the two domains of CaM are preserved in TR1C and TR2C, both in the presence and absence of Ca^{2+}. In the absence of Ca^{2+}, the two CaM fragments had identical R_H values (Table 3). The R_H values of TR1C and TR2C were not significantly affected by the presence of Ca^{2+}. Solutions containing a mixture of TR1C and TR2C showed little deviation in R_H

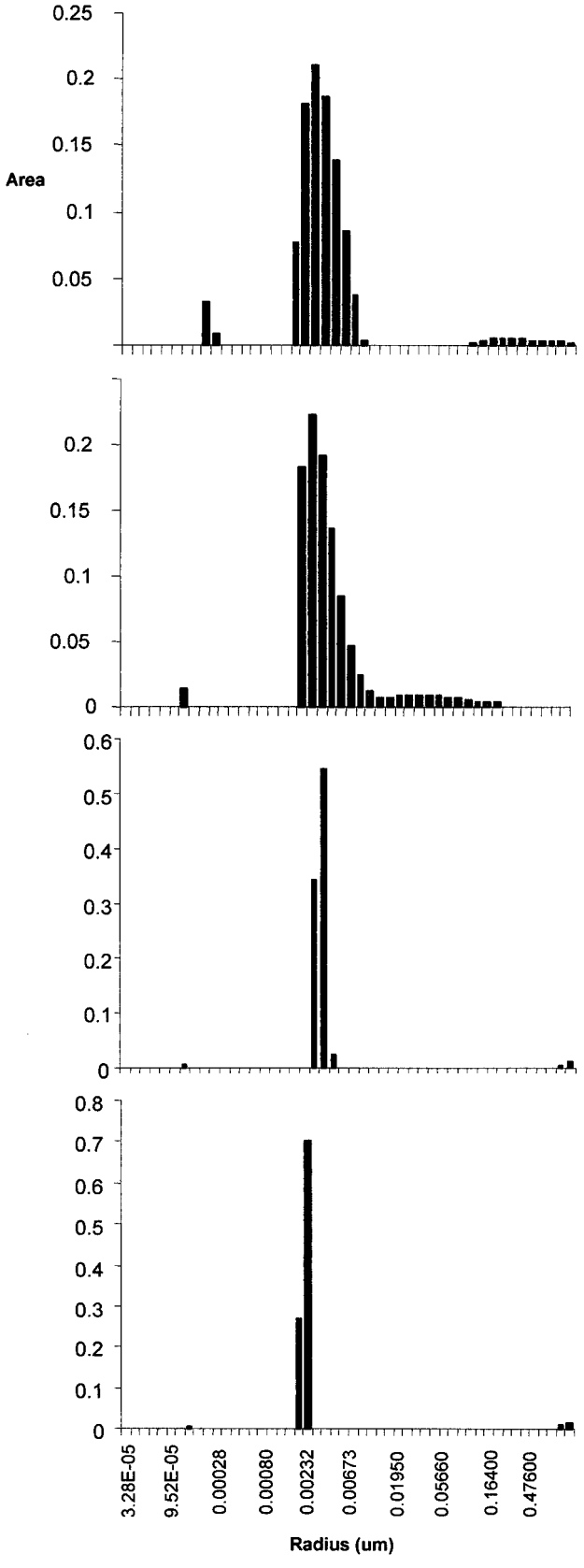

TABLE 3 Dynamic light scattering results for calmodulin fragments

	Apo		Ca^{2+}	
Fragment	RH*	(SD)	RH	(SD)
CaM	2.5	(0.1)	3.0	(0.1)
TR1C	1.8	(0.3)	2.0	(0.1)
TR2C	1.8	(0.3)	1.7	(0.2)
TR1C/TR2C	1.8	(0.3)	2.0	(0.1)
CaM/CaMKI	2.5	(0.1)	2.2	(0.1)
With CaMKI	1.6	(0.2)	2.2	(0.1)

*RH, hydrodynamic radius (nm); SD, standard deviation.

values compared to the values for the individual fragments, both in the presence and absence of Ca^{2+}. These DLS results indicate that TR1C and TR2C do not interact in solution. However, subsequent addition of the CaMKI peptide to TR1C and TR2C in the presence of Ca^{2+} resulted in an identical R_H to that of the complex formed between intact Ca^{2+}-CaM and CaMKI (2.2 nm, Table 3). NMR solution studies by Yuan et al. (2001, 2002) indicate that a globular complex is formed when TR1C and TR2C interact with various peptides in the presence of Ca^{2+}, although this interaction is not as tight as the one formed with intact Ca^{2+}-CaM. The DLS results in Table 3 are consistent with the formation of a globular complex between the two CaM fragments and the CaMKI peptide, in the presence of Ca^{2+}.

CONCLUSION

In conclusion, it is evident that DLS can be used very effectively to obtain information about the size of proteins such as calmodulin, their fragments and their complexes in solution and thus any shape or conformational changes resulting from their binding can be detected. Additionally, this work demonstrates the utility of DLS as a rapid screen for CaM target peptides, and it can be inferred that DLS would work well for other proteins that undergo dramatic conformational changes upon binding of target peptides. Results obtained for apo-CaM, Ca^{2+}-CaM and skMLCK peptide–Ca^{2+}-CaM using DLS were closely comparable to those obtained for these samples using SAXS. The new data presented in this work, which extend on the reported SAXS studies, demonstrated that all of the peptides studied induced a globularization of calcium-calmodulin to varying extents, and that none induced a significant change in apo-CaM. Collectively, these results are consistent with many previous studies performed using x-ray crystallography, NMR, SAXS, infrared and circular dichroism spectroscopy

FIGURE 4 Size distribution histogram for: (*A*) apo-CaM and one equivalent of PGD peptide; (*B*) Ca^{2+}-CaM and one equivalent of PGD peptide; (*C*) Ca^{2+}-CaM and two equivalents of PGD peptide; (*D*) Ca^{2+}-CaM and three equivalents of PGD peptide.

(Ikura et al., 1992; Meador et al., 1992, 1993; Zhang et al., 1994a, 1995b; Yuan et al., 1995, 1999b), and also offered new insights into the interactions of the peptides with CaM. It was also shown that the two CaM fragments, TR1C and TR2C, do not interact in solution both in the presence and absence of Ca^{2+}. However, the identical R_H resulting from the addition of the CaMKI peptide to either a solution of intact Ca^{2+}-CaM or to a solution containing Ca^{2+}, TR1C, and TR2C support the prediction that a globular complex is being formed between the two fragments and the peptide. This has been seen in NMR solution studies of TR1C and TR2C in the presence of different CaM target peptides and Ca^{2+} (Yuan et al., 2001, 2002).

Clearly, DLS presents itself as a rapid and useful method to screen for and compare the binding of a large number of CaM target peptides. Also, with the addition of information provided by various other techniques such as NMR, fluorescence, infrared, and circular dichroism spectroscopy, DLS can effectively be used to obtain a more complete qualitative picture of how the conformation of CaM changes upon binding to its target proteins or peptides. The result is a more thorough understanding of how CaM activates its targets. SAXS can potentially provide complementary information regarding the size and shape of macromolecules because it provides a measure of the maximum distance between two atoms of the molecule in solution, as opposed to the indirect R_H values obtained via DLS (Yoshino et al., 1993; Trewhella, 1997; Trewhella and Krueger, 2002). Several recent studies have also used DLS to obtain structural and conformational information about other proteins and their complexes (Cruzylo et al., 1997; Yajima et al., 1998; Zarutskie et al., 1999). The success of DLS in the analysis of CaM–peptide complexes and the wealth of rudimentary structural information that can be obtained make DLS a valuable technique for studies of not only other CaM–target peptide interactions, but for other macromolecules that undergo large-scale conformational changes upon ligand binding.

We wish to thank Dr. H. Ouyang and Dr. R. Brokx for advice on calmodulin purification and characterization.

This work was supported by operating grants from the Alberta Heart and Stroke Foundation (to H.J.V.). The instrument was purchased through a grant from the Alberta Heritage Foundation for Medical Research (AHFMR) (to L.W.T.). L.W.T. and H.J.V. are the recipients of Scholarship and Scientist Awards, respectively, from AHFMR.

REFERENCES

Babu, Y. S., C. E. Bugg, and W. J. Cook. 1988. Structure of calmodulin refined at 2 · 2 Å resolution. *J. Mol. Biol.* 204:191–204.

Barbato, G., M. Ikura, L. E. Kay, R. W. Pastor, and A. Bax. 1992. Backbone dynamics of calmodulin studied by ^{15}N NMR. *Biochemistry.* 31:5269–5278.

Brokx, R. D., M. M. Lopez, H. J. Vogel, and G. I. Makhatadze. 2001. Energetics of target peptide binding by calmodulin reveals different modes of binding. *J. Biol. Chem.* 276:14083–14091.

Crivici, A., and M. Ikura. 1995. Molecular and structural basis of target recognition by calmodulin. *Annu. Rev. Biophys. Biomol. Struct.* 24: 85–116.

Cruzylo, E. A., T. Hellweg, E. Eimer, and R. Dabrowska. 1997. The size and shape of caldesmon and its fragments in solution studied by dynamic light scattering and hydrodynamic model calculations. *Biophys. J.* 172: 835–842.

Fabian, H., T. Yuan, H. J. Vogel, and H. H. Mantsch. 1996. Comparative analysis of the amino- and carboxy-terminal domains of calmodulin by Fourier transform infrared spectroscopy. *Eur. Biophys. J.* 24:195–201.

Gellman, S. H. 1991. The role of methionine residues in the sequence-independent recognition of nonpolar protein surfaces. *Biochemistry.* 30:6633–6636.

Gomes, A., M. Barnes, and H. J. Vogel. 2000. Spectroscopic characterization of the interaction between calmodulin dependent protein kinase I and calmodulin. *Arch. Biochem. Biophys.* 379:28–36.

Heidorn, D. B., and J. Trewhalla. 1988. Comparison of the crystal and solution structures of calmodulin and troponin C. *Biochemistry.* 27: 909–915.

Ikura, M. 1996. Calcium binding and conformational response in EF-hand proteins. *Trends Biochem. Sci.* 21:14–17.

Ikura, M., G. M. Clore, A. M. Gronenborn, G. Zhu, C. B. Klee, and A. Bax. 1992. Solution structure of a calmodulin-target peptide complex by multidimensional NMR. *Science.* 256:632–638.

Izumi, Y., S. Kuwamoto, Y. Jinbo, and H. Yoshino. 2001. Increase in the molecular weight and radius of gyration of apocalmodulin induced by binding of target peptide: evidence for complex formation. *FEBS Lett.* 495:126–130.

James, P., T. Vorherr, and E. Carafoli. 1995. Calmodulin-binding domains: just two faced or multifaced? *Trends Biochem. Sci.* 20:38–42.

Kataoka, M., J. F. Head, A. Persechini, R. H. Kretsinger, and D. M. Engelman. 1991. Small-angle x-ray scattering studies of calmodulin mutants with deletions in the linker region of the central helix indicate that the linker region retains a predominantly α-helical conformation. *Biochemistry.* 30:1188–1192.

Kataoka, M., J. F. Head, T. Vorherr, J. Krebs, and E. Carafoli. 1991. Small-angle x-ray scattering study of calmodulin bound to two peptides corresponding to parts of the calmodulin-binding domain of the plasma membrane Ca^{2+} pump. *Biochemistry.* 30:6247–6251.

Kranz, J. K., E. K. Lee, A. C. Nairn, and A. J. Wand. 2002. A direct test of the reductionist approach to structural studies of calmodulin activity. *J. Biol. Chem.* 277:16351–16354.

Krueger, J. K., S. C. Gallagher, C. A. Wang, and J. Trewhella. 2000. Calmodulin remains extended upon binding to smooth muscle caldesmon: a combined small-angle scattering and Fourier transform infrared spectroscopy study. *Biochemistry.* 39:3979–3987.

Kuboniwa, H., N. Tjandra, S. Grzesiek, H. Ren, C. B. Klee, and A. Bax. 1995. Solution structure of calcium-free calmodulin. *Nat. Struct. Biol.* 2:768–776.

Meador, W. E., A. R. Means, and F. A. Quiocho. 1992. Target enzyme recognition by calmodulin: 2.4 Å structure of a calmodulin-peptide complex. *Science.* 257:1251–1255.

Meador, W. E., A. R. Means, and F. A. Quiocho. 1993. Modulation of calmodulin plasticity in molecular recognition on the basis of x-ray structures. *Science.* 262:1718–1721.

Murphy, R. M. 1997. Static and dynamic light scattering of biological macromolecules: what can we learn? *Curr. Opin. Biotechn.* 8:25–30.

O'Neil, K. T., and W. F. DeGrado. 1990. How calmodulin binds its targets: sequence independent recognition of amphiphilic α-helices. *Trends Biochem. Sci.* 15:59–64.

Schumacher, M. A., A. F. Rivard, H. P. Bachinger, and J. P. Adelman. 2001. Structure of the gating domain of a Ca^{2+}-activated K^+ channel complexed with Ca^{2+}/calmodulin. *Nature.* 410:1120–1124.

Seaton, B. A., J. F. Head, D. M. Engelman, and F. M. Richards. 1985. Calcium-induced increase in the radius of gyration and maximum dimension of calmodulin measured by small-angle x-ray scattering. *Biochemistry.* 24:6740–6743.

Squire, P. G., and M. E. Himmel. 1979. Hydrodynamics and protein hydration. *Arch. Biochem. Biophys.* 196:165–177.

Thulin, E., A. Andersson, T. Drakenberg, S. Forsen, and H. J. Vogel. 1984. Metal ion and drug binding to proteolytic fragments of calmodulin: proteolytic, cadmium-113, and proton nuclear magnetic resonance studies. *Biochemistry.* 23:1862–1870.

Trewhella, J. 1997. Insights into biomolecular function from small-angle scattering. *Curr. Opin. Struct. Biol.* 7:702–708.

Trewhella, J., D. K. Blumenthal, S. E. Rokop, and P. A. Seeger. 1990. Small angle scattering studies show distinct conformations of calmodulin in its complexes with two peptides based on the regulatory domain of the catalytic subunit of phosphorylase kinase. *Biochemistry.* 29: 9316–9324.

Trewhella, J., and J. K. Krueger. 2002. Small angle solution scattering reveals information on conformational dynamics in calcium binding proteins and in their interactions with regulatory targets. *In* Methods of Molecular Biology. Vol. 173. H. J. Vogel, editor. Humana Press, Totowa, NJ. 137–160.

van Holde, K. E., W. C. Johnson, and P. S. Ho. 1998. Principles of Physical Biochemistry. Prentice-Hall, Inc., Upper Saddle River, NJ. 657.

Vogel, H. J. 1994. Calmodulin: a versatile calcium mediator protein. *Biochem. Cell Biol.* 72:357–376.

Vogel, H. J., L. Lindahl, and E. Thulin. 1983. Calcium-dependent hydrophobic interaction chromatography of calmodulin, troponin C, and their proteolytic fragments. *FEBS Lett.* 157:241–246.

Vogel, H. J., and M. Zhang. 1995. Protein engineering and NMR studies of calmodulin. *Mol. Cell. Biochem.* 149/150:3–15.

Wang, E., S. Zhuang, J. Kordowska, Z. Grabarek, and C.-L. A. Wang. 1997. Calmodulin binds to caldesmon in an antiparallel manner. *Biochemistry.* 36:15026–15034.

Yajima, H., H. Yamamoto, M. Nagaoka, K. Nakazato, T. Ishii, and N. Niimura. 1998. Small-angle neutron scattering and dynamic light scattering studies of N- and C-terminal fragments of ovotransferrin. *Biochim. Biophys. Acta.* 1381:68–76.

Yoshino, H., Y. Izumi, K. Sakai, H. Takezawa, I. Matsuura, H. Maekawa, and M. Yazawa. 1996. Solution x-ray scattering data show structural differences between yeast and vertebrate calmodulin: implications for structure/function. *Biochemistry.* 35:2388–2393.

Yoshino, H., M. Wakita, and Y. Izumi. 1993. Calcium-dependent changes in structure of calmodulin with substance P. *J. Biol. Chem.* 268: 12123–12128.

Yuan, T., T. A. Mietzner, R. C. Montelaro, and H. J. Vogel. 1995. Characterization of the calmodulin binding domain of SIV transmembrane glycoprotein by NMR and CD spectroscopy. *Biochemistry.* 34: 10690–10696.

Yuan, T., H. Ouyang, and H. J. Vogel. 1999a. Surface exposure of the methionine side chains of calmodulin in solution. A nitroxide spin label and two-dimensional NMR study. *J. Biol. Chem.* 274:8411–8420.

Yuan, T., S. Tencza, T. A. Mietzner, R. C. Montelaro, and H. J. Vogel. 2001. Calmodulin binding properties of peptide analogs and fragments of the calmodulin binding domain of SIV transmembrane glycoprotein. *Biopolymers.* 58:50–62.

Yuan, T., and H. J. Vogel. 1998. Calcium–calmodulin-induced dimerization of the carboxyl-terminal domain from petunia glutamate decarboxylase. A novel calmodulin–peptide interaction motif. *J. Biol. Chem.* 273:30328–30335.

Yuan, T., M. P. Walsh, C. Sutherland, H. Fabian, and H. J. Vogel. 1999b. Calcium-dependent and -independent interactions of the calmodulin-binding domain of cyclic nucleotide phosphodiesterase with calmodulin. *Biochemistry.* 38:1446–1455.

Zarutskie, J. A., A. K. Sato, M. M. Rushe, I. C. Chan, A. Lomakin, G. B. Benedek, and L. J. Stern. 1999. A conformational change in the human major histocompatibility complex protein HLA-DR1 induced by peptide binding. *Biochemistry.* 38:5878–5887.

Zhang, M., H. Fabian, H. H. Mantsch, and H. J. Vogel. 1994a. Isotope-edited FTIR spectroscopy studies of calmodulin's interaction with its target peptides. *Biochemistry.* 33:10883–10888.

Zhang, M., T. Tanaka, and M. Ikura. 1995a. Calcium-induced conformational transition revealed by the solution structure of apo calmodulin. *Nat. Struct. Biol.* 2:758–767.

Zhang, M., and H. J. Vogel. 1993. Determination of the sidechain pKa values of the lysine residues in calmodulin. *J. Biol. Chem.* 268: 22420–22428.

Zhang, M., and H. J. Vogel. 1994. Characterization of the calmodulin-binding domain of rat cerebellar nitric oxide synthase. *J. Biol. Chem.* 269:981–985.

Zhang, M., T. Yuan, J. Aramini, and H. J. Vogel. 1995b. A multimolecular NMR study of the interaction between calmodulin and its binding domain of rat cerebellum nitric oxide synthase. *J. Biol. Chem.* 270: 20901–20907.

Zhang, M., T. Yuan, and H. J. Vogel. 1993. A peptide analog of the calmodulin-binding domain of myosin light chain kinase adopts an α-helical structure in aqueous trifluoroethanol. *Protein Sci.* 2:1931–1937.

Zhou, N., T. Yuan, A. S. Mak, and H. J. Vogel. 1997. NMR studies of caldesmon–calmodulin interactions. *Biochemistry.* 36:2817–2825.